CP transformed mixed $\mu\tau$ antisymmetry for neutrinos and its consequences

Roopam Sinha,[1,*] Probir Roy,[2,†] and Ambar Ghosal[1,‡]

[1]*Astroparticle Physics and Cosmology Division Saha Institute of Nuclear Physics, HBNI, Kolkata 700064, India*

[2]*Center for Astroparticle Physics and Space Science Bose Institute, Kolkata 700091, India*

(Received 26 September 2018; published 20 February 2019)

We propose a complex extension of mixed $\mu\tau$ antisymmetry in the neutrino Majorana mass matrix M_ν. This can be implemented in the Lagrangian by a generalized *CP* transformation (labeled by a mixing parameter θ) on the left-chiral flavor neutrino fields. We investigate its implications for leptonic *CP* violation and neutrino phenomenology in general. Interestingly, the $\mu\tau$ mixing parameter θ gets correlated with the Dirac *CP* phase δ and the atmospheric mixing angle θ_{23} through an analytical relation. In general, for arbitrary θ, both θ_{23} and δ are nonmaximal. We discuss the corresponding results for the *CP* asymmetry parameter $A_{\mu e}$ in neutrino oscillation experiments. For a nonmaximal δ, one of the two Majorana phases is different from 0 or π, thereby leading to nonvanishing Majorana *CP* violation with observable consequences for the neutrinoless double-beta ($\beta\beta0\nu$) decay process. We numerically work out in detail the predictions for that process in relation to various ongoing and forthcoming experiments. We also work out the predictions of our scheme on flavor flux ratios at neutrino telescopes. While exact *CP*-transformed $\mu\tau$ interchange antisymmetry ($\theta = \pi/2$) leads to an exact equality among those ratios, taking the value 0.5, a tiny deviation can cause a drastic change in them. Careful measurements of these flux ratios in the future will further constrain the parameter θ.

DOI: 10.1103/PhysRevD.99.033009

I. INTRODUCTION

The theoretical origin of the masses, mixing pattern and *CP* properties [1] of the three light neutrinos continues to be an open question. Experimentally, the three mixing angles and the two mass-squared differences are already known to a reasonably good accuracy while a fairly tight cosmological upper bound [2] of 0.17 eV exists on the sum of the three masses. The solar mixing angle θ_{12} is close to 33.62° while the reactor mixing angle θ_{13} is known to be largely nonzero and approximately equal to 8.5°. The latest update of the combined global fit of neutrino oscillation data from experiments such as T2K [3], NOνA [4], MINOS [5], and RENO [6] prefers a near maximal value of the atmospheric mixing angle θ_{23}. Although the octant of θ_{23} is yet unknown the best-fit values are $\theta_{23} = 47.2°$ for normal ordering (NO) and $\theta_{23} = 48.1°$ for inverse ordering (IO), where the higher octant preferred for both. For the Dirac *CP* phase δ, the current best-fit values are close to 234° for NO and 278° for IO. Its *CP*-conserving values (i.e., $\delta = 0$, π) are allowed at slightly above 1σ and $\delta = \pi/2$ is disfavored at 99% C.L. [7] In this scenario, $\delta = 3\pi/2$ and any slight deviation from it are still permitted as interesting possibilities. Insofar as the precision measurements of δ and θ_{23} are concerned, we are at a decisive moment in time since the neutrino mass models that survive current phenomenological constraints and predict a cobimaximal mixing ($\theta_{23} = \pi/4$, $\delta = \pi/2$ or $3\pi/2$) [8] could be subjected to stringent experimental tests. Also, the nature of the light neutrinos, whether Dirac or Majorana, remains shrouded in mystery. Perhaps future experiments will resolve the matter through a signature of the neutrinoless double-β decay process which crucially depends upon the values of the two Majorana phases of the neutrinos.

Let us first consider various discrete flavor symmetries in the $\mu\tau$ sector of neutrinos which have been proposed to understand the observed pattern of neutrino mixing. One class of such symmetries entails $\mu\tau$ mixing [9], to wit an invariance under the transformation

$$\nu_{Ll} \to G^{\theta}_{lm}\nu_{Lm}. \tag{1.1}$$

Here G^θ is a generator of a residual $\mathbb{Z}_2$ symmetry affecting the mixing, l, m span the flavor indices e, μ, τ while the subscript L denotes left-chiral flavor neutrino fields. In neutrino flavor space G^θ has the generic form

*roopam.sinha@saha.ac.in
†probirrana@gmail.com
‡ambar.ghosal@saha.ac.in

$$G^\theta = \begin{pmatrix} -1 & 0 & 0 \\ 0 & -\cos\theta & \sin\theta \\ 0 & \sin\theta & \cos\theta \end{pmatrix}, \tag{1.2}$$

where θ is a mixing parameter. The location of the minus sign in Eq. (1.2) is because of our convention of choosing $\det G^\theta$ to be $+1$ without any loss of generality. The special case of Eq. (1.1) for $\theta = \pi/2$ has been known in the literature as $\mu\tau$ interchange symmetry which can stem from some high-energy flavor symmetry group such as S_4 [10]. Further, a number of studies [11] have investigated the phenomenological consequences of Eq. (1.1). It has been found that the reactor mixing angle θ_{13} vanishes if one imposes the symmetry (1.1) with Eq. (1.2). Since this possibility has now been excluded at more than 10σ [12], this symmetry has to be discarded.

An interesting variant of Eq. (1.1) is the symmetry of CP-transformed [13] $\mu\tau$ mixing, as proposed in Ref. [14]. This is an invariance of the neutrino Majorana mass term under the transformation

$$\nu_{Ll} \to iG^\theta_{lm}\gamma^0\nu^C_{Lm} \tag{1.3}$$

with G^θ as in Eq. (1.2) and $\nu^C_{Ll} = C\overline{(\nu_{Ll})}^T$. The corresponding phenomenological consequences have been studied [14]. A different approach using the idea of the littlest $\mu\tau$ seesaw [15] has also been recently proposed allowing slight deviations from maximal θ_{23} and maximal Dirac CP violation. It should be noted that the $\theta \to \pi/2$ limit of Eq. (1.3), referred to as a CP-transformed $\mu\tau$ interchange symmetry ($CP^{\mu\tau}$), had earlier been extensively studied [8] and avoids the problem of a vanishing reactor angle. However, it predicts maximal values for the atmospheric mixing angle θ_{23} and the Dirac CP phase δ, namely $\theta_{23} = \pi/4$ and $\cos\delta = 0$. Such a possibility, though still allowed by current experimental limits, is being challenged by ongoing and forthcoming precision measurements of these quantities. In case the maximality of either quantity is ruled out in the future, CP-transformed $\mu\tau$ interchange symmetry will be excluded.

In this paper, we propose a complex antisymmetric extension of Eq. (1.3) using a $\mathbb{Z}_4$ generator $\mathcal{G}^\theta = iG^\theta$

$$\nu_{Ll} \to i\mathcal{G}^\theta_{lm}\gamma^0\nu^C_{Lm}. \tag{1.4}$$

A special case of such an invariance with $\theta = \pi/2$ was proposed by some of us in Ref. [16]. The latter avoids the problem of a vanishing θ_{13} but leads to maximal values of the atmospheric mixing angle θ_{23} and the Dirac CP phase δ. As explained above, these results may not survive for much longer. In this situation our proposal of an invariance under Eq. (1.4) with $\theta \neq \pi/2$ assumes a special significance since it allows any arbitrary nonzero value of θ_{13} and nonmaximal θ_{23} depending on the parameter θ. Since in this work we concentrate on the low-energy phenomenological consequences, we start from the effective field transformation (1.4) without providing a larger symmetry that embeds it. In the case of CP combined with a flavor symmetry, a nontrivial challenge would be to satisfy the consistency conditions [13]. Now real a $\mu\tau$ interchange antisymmetry [17] has been shown to arise in a class of explicit models with larger discrete symmetries including $\mathbb{Z}_4$ while Ref. [18] discussed that the neutrino (Majorana) mass matrix can enjoy pure flavor antisymmetry under some discrete subgroups contained in A_5. Again, a real mixed $\mu\tau$ symmetry [19] arises in a model where the charged lepton and neutrino mass matrices are invariant under specific residual symmetries contained in the finite discrete subgroups of $O(3)$. The latter work provided an explicit model based on A_5 maintaining the mixed $\mu\tau$ symmetry. However, such a demonstration is lacking in the literature for the corresponding CP-transformed (complex extended) cases.

The rest of the paper is organized as follows. Section II deals with the symmetries of the neutrino Majorana mass matrix M_ν and the most general parametrization of M_ν that is invariant under Eq. (1.4). Section III contains the evaluation of Majorana phases and a definite relation between the leptonic Dirac CP phase and the atmospheric mixing angle θ_{23} that involves the $\mu\tau$ mixing parameter θ. In Sec. IV a numerical analysis of our proposal is presented utilizing neutrino oscillation data; this entails the extraction of the allowed parameter space and the prediction of light neutrino masses. It consists of three subsections. The first considers neutrinoless double-beta decay; the second includes the range of variation of the CP asymmetry parameter $A_{\mu e}$ in experiments such as T2K, NoνA and DUNE for both types of mass ordering; and the variation of flavor flux ratios at neutrino telescopes is considered in the third. In Sec. V we summarize the results of our analysis.

II. COMPLEX MIXED $\mu\tau$ ANTISYMMETRY OF THE NEUTRINO MAJORANA MASS MATRIX

The effective neutrino Majorana mass term in the Lagrangian density reads

$$-\mathcal{L}^\nu_{\text{mass}} = \frac{1}{2}\overline{\nu^C_{Ll}}(M_\nu)_{lm}\nu_{Lm} + \text{H.c.} \tag{2.1}$$

where $\nu^C_{Ll} = C\overline{(\nu_{Ll})}^T$ and the subscripts l, m span the lepton flavor indices e, μ, τ while the subscript L denotes left-chiral neutrino fields. Here, M_ν is a complex symmetric matrix ($M^*_\nu \neq M_\nu = M^T_\nu$) in lepton flavor space. It can be diagonalized by a similarity transformation with a unitary matrix U:

$$U^T M_\nu U = M^d_\nu \equiv \text{diag}(m_1, m_2, m_3). \tag{2.2}$$

Here $m_i (i = 1, 2, 3)$ are real and we assume that $m_i \geq 0$. Without any loss of generality, we work in the diagonal basis of the charged leptons so that U can be related to the Pontecorvo-Maki-Nakagawa-Sakata (PMNS) matrix $U_{\rm PMNS}$:

$$U = P_\phi U_{\rm PMNS} \equiv P_\phi \begin{pmatrix} c_{12}c_{13} & e^{\frac{i\alpha}{2}} s_{12}c_{13} & s_{13}e^{-i(\delta-\frac{\beta}{2})} \\ -s_{12}c_{23} - c_{12}s_{23}s_{13}e^{i\delta} & e^{\frac{i\alpha}{2}}(c_{12}c_{23} - s_{12}s_{13}s_{23}e^{i\delta}) & c_{13}s_{23}e^{i\frac{\beta}{2}} \\ s_{12}s_{23} - c_{12}s_{13}c_{23}e^{i\delta} & e^{\frac{i\alpha}{2}}(-c_{12}s_{23} - s_{12}s_{13}c_{23}e^{i\delta}) & c_{13}c_{23}e^{i\frac{\beta}{2}} \end{pmatrix}, \tag{2.3}$$

where $P_\phi = \text{diag}(e^{i\phi_1}, e^{i\phi_2}e^{i\phi_3})$ is an unphysical diagonal phase matrix and $c_{ij} \equiv \cos\theta_{ij}$, $s_{ij} \equiv \sin\theta_{ij}$ with the mixing angles $\theta_{ij} \in [0, \pi/2]$. We follow the Particle Data Group (PDG) convention [20] but denote our Majorana phases by α and β instead of α_{21} and α_{31}. CP violation enters through nontrivial values of the Dirac phase δ and of the Majorana phases α, β with δ, α, $\beta \in [0, 2\pi]$.

The effect of our proposed invariance under Eq. (1.4) on the neutrino Majorana mass matrix would be

$$\mathcal{G}^{\theta T} M_\nu \mathcal{G}^\theta = -M_\nu^*. \tag{2.4}$$

$\mathcal{G}^\theta$ in Eq. (2.4) is given by iG^θ where G^θ was defined in Eq. (1.2). In flavor space, the most generally parametrized 3×3 complex symmetric mass matrix obeying Eq. (2.4) is given by

$$M_\nu^{CP\theta A} = \begin{pmatrix} ix & a_1 + ia_2 & a_1 t_{\frac{\theta}{2}}^{-1} - ia_2 t_{\frac{\theta}{2}} \\ a_1 + ia_2 & y_1 + iy_2 & y_1 c_\theta s_\theta^{-1} + ic \\ a_1 t_{\frac{\theta}{2}}^{-1} - ia_2 t_{\frac{\theta}{2}} & y_1 c_\theta s_\theta^{-1} + ic & -y_1 + i(y_2 + 2cc_\theta s_\theta^{-1}) \end{pmatrix}, \tag{2.5}$$

where $c_\theta \equiv \cos\theta$, $s_\theta \equiv \sin\theta$ and $t_{\frac{\theta}{2}} \equiv \tan\frac{\theta}{2}$. In Eq. (2.5), there are seven real free parameters x, $a_{1,2}$, c, y_1, y_2 and θ. As expected, the limit $\theta \to \pi/2$ gives back the mass matrix $M_\nu^{CP\mu\tau A}$ which is invariant under CP-transformed $\mu\tau$ interchange antisymmetry [16], namely

$$M_\nu^{CP\mu\tau A} = \begin{pmatrix} ix & a_1 + ia_2 & a_1 - ia_2 \\ a_1 + ia_2 & y_1 + iy_2 & ic \\ a_1 - ia_2 & ic & -y_1 + iy_2 \end{pmatrix}. \tag{2.6}$$

It should be emphasized that complex mixed $\mu\tau$ antisymmetry, which can be abbreviated as $CP^{\theta\mu\tau A}$ and gets generated by $\mathcal{G}^\theta$, must now be broken in the charged lepton sector. This is because a nonzero Dirac CP violation is equivalent to the criterion

$$\text{Tr}[H_\nu, H_\ell]^3 \neq 0, \tag{2.7}$$

where H_ν and H_ℓ are two Hermitian matrices defined as $H_\ell = M_\ell^\dagger M_\ell$, M_ℓ (being the charged lepton mass matrix) and $H_\nu = M_\nu^\dagger M_\nu$. [21]. A common CP symmetry $\mathcal{G}_{CP}$ would imply

$$\mathcal{G}_{CP}^T H_\nu^T \mathcal{G}_{CP}^* = H_\nu, \qquad \mathcal{G}_{CP}^T H_\ell^T \mathcal{G}_{CP}^* = H_\ell. \tag{2.8}$$

From Eq. (2.8) it follows that $\text{Tr}[H_\nu, H_\ell]^3 = 0$ which leads to $\sin\delta = 0$ i.e., a vanishing Dirac CP violation. As mentioned earlier, this is disfavored by current experiments.

III. NEUTRINO MIXING ANGLES AND PHASES

Equations (2.2) and (2.4) together imply [8] that

$$\mathcal{G}^\theta U^* = U\tilde{d} \tag{3.1}$$

where $\tilde{d}_{ij} = \pm\delta_{ij}$. Next, we take $\tilde{d} = \text{diag}(\tilde{d}_1, \tilde{d}_2, \tilde{d}_3)$ where each $\tilde{d}_i$ $(i = 1, 2, 3)$ is either $+1$ or -1. Equation (3.1) can be explicitly written as

$$\begin{pmatrix} -i & 0 & 0 \\ 0 & -ic_\theta & is_\theta \\ 0 & is_\theta & ic_\theta \end{pmatrix} \begin{pmatrix} U_{e1}^* & U_{e2}^* & U_{e3}^* \\ U_{\mu1}^* & U_{\mu2}^* & U_{\mu3}^* \\ U_{\tau1}^* & U_{\tau2}^* & U_{\tau3}^* \end{pmatrix} = \begin{pmatrix} \tilde{d}_1 U_{e1} & \tilde{d}_2 U_{e2} & \tilde{d}_3 U_{e3} \\ \tilde{d}_1 U_{\mu1} & \tilde{d}_2 U_{\mu2} & \tilde{d}_3 U_{\mu3} \\ \tilde{d}_1 U_{\tau1} & \tilde{d}_1 U_{\tau2} & \tilde{d}_1 U_{\tau3} \end{pmatrix}. \tag{3.2}$$

Equation (3.2) leads to nine independent relations corresponding to the three rows:

$$
\begin{aligned}
-iU_{e1}^{*} &= \tilde{d}_1 U_{e1}, \qquad -iU_{e2}^{*} = \tilde{d}_2 U_{e2}, \qquad -iU_{e2}^{*} = \tilde{d}_3 U_{e3}, \\
-iU_{\mu 1}^{*} c_\theta + iU_{\tau 1}^{*} s_\theta &= \tilde{d}_1 U_{\mu 1}, \qquad -iU_{\mu 2}^{*} c_\theta + iU_{\tau 2}^{*} s_\theta = \tilde{d}_2 U_{\mu 2}, \qquad -iU_{\mu 3}^{*} c_\theta + iU_{\tau 3}^{*} s_\theta = \tilde{d}_3 U_{\mu 3}, \\
iU_{\mu 1}^{*} s_\theta + iU_{\tau 1}^{*} c_\theta &= \tilde{d}_1 U_{\tau 1}, \qquad iU_{\mu 2}^{*} s_\theta + iU_{\tau 2}^{*} c_\theta = \tilde{d}_2 U_{\tau 2}, \qquad iU_{\mu 3}^{*} s_\theta + iU_{\tau 3}^{*} c_\theta = \tilde{d}_3 U_{\tau 3}. \qquad (3.3)
\end{aligned}
$$

In order to calculate the Majorana phases in a way that avoids unphysical phases, it is useful to construct two rephasing invariants [22]

$$I_1 = U_{e1} U_{e2}^{*}, \qquad I_2 = U_{e1} U_{e3}^{*}. \qquad (3.4)$$

Using the relations in the first row of Eq. (3.3), we obtain

$$I_1 = \tilde{d}_1 \tilde{d}_2 U_{e1}^{*} U_{e2}, \qquad I_2 = \tilde{d}_1 \tilde{d}_2 U_{e1}^{*} U_{e3}. \qquad (3.5)$$

On inserting the two different expressions for $I_{1,2}$, in Eqs. (3.4) and (3.5), we find that

$$c_{12} s_{12} c_{13}^2 e^{-i\alpha/2} = \tilde{d}_1 \tilde{d}_2 c_{12} s_{12} c_{13}^2 e^{i\alpha/2} \qquad (3.6)$$

and

$$c_{12} s_{13} c_{13} e^{i(\delta - \beta/2)} = \tilde{d}_1 \tilde{d}_3 c_{12} s_{13} c_{13} e^{-i(\delta - \beta/2)}. \qquad (3.7)$$

From Eqs. (3.6) and (3.7), it follows that

$$e^{i\alpha} = \tilde{d}_1 \tilde{d}_2, \qquad e^{2i(\delta - \beta/2)} = \tilde{d}_1 \tilde{d}_3, \qquad (3.8)$$

i.e., either $\alpha = 0$ or $\alpha = \pi$, and either $\beta = 2\delta$ or $\beta = 2\delta - \pi$. In other words, the Majorana phases can have four possible pairs of values for a given value of δ. From the absolute square of the third relation in the third row of Eq. (3.5), we obtain

$$|U_{\tau 3}|^2 = (U_{\mu 3}^{*} s_\theta + U_{\tau 3}^{*} c_\theta)(U_{\mu 3} s_\theta + U_{\tau 3} c_\theta) \qquad (3.9)$$

which implies that

$$\cot 2\theta_{23} = \cot\theta \cos(\phi_2 - \phi_3) \qquad (3.10)$$

which reduces to $\theta_{23} \to \pi/4$ in the $\mu\tau$ interchange limit $\theta \to \pi/2$, as expected. Taking the absolute square of the second relation in the third row of Eq. (3.3), and eliminating the unphysical phase difference $\phi_2 - \phi_3$, we obtain

$$\sin\delta = \pm \sin\theta / \sin 2\theta_{23}. \qquad (3.11)$$

This result was originally derived in Ref. [14] which proposed a CP-transformed mixed $\mu\tau$ symmetry for neutrinos. Equation (3.11), as expected, reproduces the result $\sin\delta = \pm 1$ (equivalently, $\cos\delta = 0$) in the $\mu\tau$ interchange limit $\theta = \pi/2$ and $\theta_{23} = \pi/4$. Note also that, if the unphysical phase combination $\phi_2 - \phi_3$ is put equal to zero, $\cot 2\theta_{23}$ becomes equal to $\cot\theta$ and $\cos\delta$ vanishes i.e., leptonic Dirac CP violation becomes maximal. However, this is not the case in general. We should also mention that another relation between δ and θ_{13} was obtained recently in Ref. [23].

IV. NUMERICAL ANALYSIS

In order to demonstrate the phenomenological viability of our theoretical proposal we present a numerical analysis of its consequences in substantial detail. It is organized as follows. In Table I, we display the 3σ ranges of neutrino mixing angles and mass-squared differences obtained from globally fitted neutrino oscillation data [7]. The allowed ranges of parameters of M_ν, CP phases and the consequent predictions on the light neutrino masses are tabulated in Tables II, III and Table IV respectively. These have been obtained by using the exact analytical formulas for the

TABLE I. Input values used in the analysis [7].

Parameter	θ_{12} degrees	θ_{23} degrees	θ_{13} degrees	Δm_{21}^2 10^{-5} $(\mathrm{eV})^2$	$\lvert\Delta m_{31}^2\rvert$ 10^{-3} $(\mathrm{eV})^2$
3σ ranges (NO)	31.42–36.05	40.3–51.5	8.09–8.98	6.80–8.02	2.399–2.593
3σ ranges (IO)	31.43–36.06	41.3–51.7	8.14–9.01	6.80–8.02	2.369–2.562
Best fit values (NO)	33.62	47.2	8.54	7.40	2.494
Best fit values (IO)	33.62	48.1	8.58	7.40	2.465

TABLE II. Output values of the parameters of M_ν.

Parameters	$x/10^{-2}$	$a_1/10^{-2}$	$a_2/10^{-2}$	$y_1/10^{-2}$	$y_2/10^{-2}$	$c/10^{-2}$	$\theta(^\circ)$
NO	−2.2–2.2	−4.5–4.5	−3.2–3.2	−3.5–3.5	−4.5–4.5	−3.5–3.5	12–174
IO	−2.5–2.5	−4.5–4.5	−0.4–0.4	−2.5–2.5	−3.5–3.5	−2.5–2.5	2–156

TABLE III. Output values of *CP* phases in the range $\beta \in [0, 2\pi]$.

Ordering	δ	$\beta = 2\delta$	$\beta = 2\delta - \pi$
NO $(\sin\delta > 0)$	[6°, 174°]	[12°, 348°]	[0°, 168°], [192°, 360°]
NO $(\sin\delta < 0)$	[186°, 354°]	[12°, 348°]	[0°, 168°], [192°, 360°]
IO $(\sin\delta > 0)$	[4°, 176°]	[8°, 352°]	[0°, 172°], [188°, 360°]
IO $(\sin\delta < 0)$	[184°, 356°]	[8°, 352°]	[0°, 172°], [188°, 360°]

TABLE IV. Predictions on the light neutrino masses.

Normal ordering $(m_3 > m_2)$			Inverted ordering $(m_3 < m_1)$		
$m_1/10^{-3}$ (eV)	$m_2/10^{-3}$ (eV)	$m_3/10^{-3}$ (eV)	$m_1/10^{-3}$ (eV)	$m_2/10^{-3}$ (eV)	$m_3/10^{-3}$ (eV)
8.4×10^{-2}–49	9–51	50–71	48–64	49–66	4.4×10^{-2}–42

mixing angles and light neutrino masses [24], the entries in Table I and the upper bound [2] of 0.17 eV on the sum of the light neutrino masses from Planck and other cosmological observations. In Fig. 1 each mass eigenvalue m_1, m_2 and m_3 is plotted against the smallest mass eigenvalue $m_{\rm min}$ for both types of mass ordering. The neutrino mass spectrum is clearly hierarchical ($m_{2,1} \gg m_3$ for NO and $m_{2,1} \ll m_3$ for IO).

Next, we discuss the numerical results of *CP*-transformed mixed $\mu\tau$ antisymmetry for neutrinoless double-beta decay, *CP* asymmetry in neutrino oscillations and flavor flux ratios at neutrino telescopes in three separate subsections.

A. Neutrinoless double-beta decay

In this subsection, we explore the predictions of our proposal for $\beta\beta0\nu$ decay. The latter is a lepton-number-violating process arising from the decay of a nucleus as

$$(A, Z) \to (A, Z+2) + 2e^- \tag{4.1}$$

characterized by the absence of any final-state neutrinos. The observation of such a decay will lead to the confirmation of the Majorana nature of the neutrinos. The half-life [25] corresponding to the above decay is given by

$$\frac{1}{T^{0\nu}_{1/2}} = G_{0\nu}|\mathcal{M}|^2|M^{ee}_\nu|^2 m_e^{-2}, \tag{4.2}$$

where $G_{0\nu}$ is the two-body phase space factor, $\mathcal{M}$ is the nuclear matrix element, m_e is the mass of the electron and M^{ee}_ν is the (1,1) element of the effective light neutrino mass matrix M_ν. In the PDG parametrization convention for $U_{\rm PMNS}$, M^{ee}_ν is given most generally by

$$M^{ee}_\nu = c^2_{12}c^2_{13}m_1 + s^2_{12}c^2_{13}m_2 e^{i\alpha} + s^2_{13}m_3 e^{i(\beta-2\delta)}. \tag{4.3}$$

In our case, Eq. (4.3) simplifies to the following four expressions for our four different possibilities:

(i) $|M^{ee}_\nu| = c^2_{12}c^2_{13}m_1 + s^2_{12}c^2_{13}m_2 + s^2_{13}m_3$ for $\alpha = 0$, $\beta = 2\delta$,

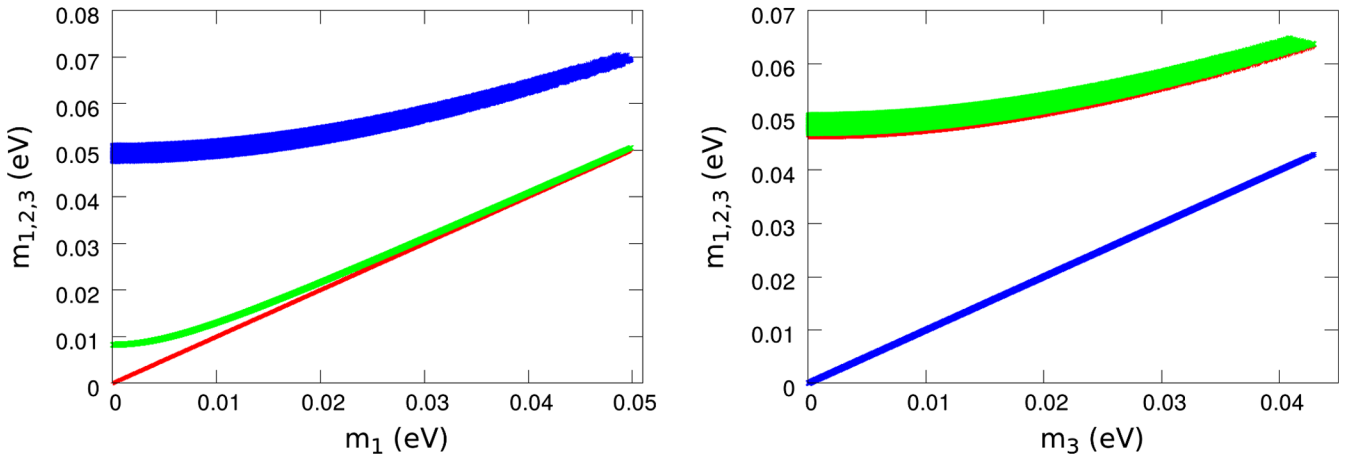

FIG. 1. Plots of $m_{1,2,3}$ for normal (left) and inverted (right) mass ordering where the lightest mass eigenvalue is plotted in the ordinate. The red, green and blue bands refer to m_1, m_2 and m_3 respectively.

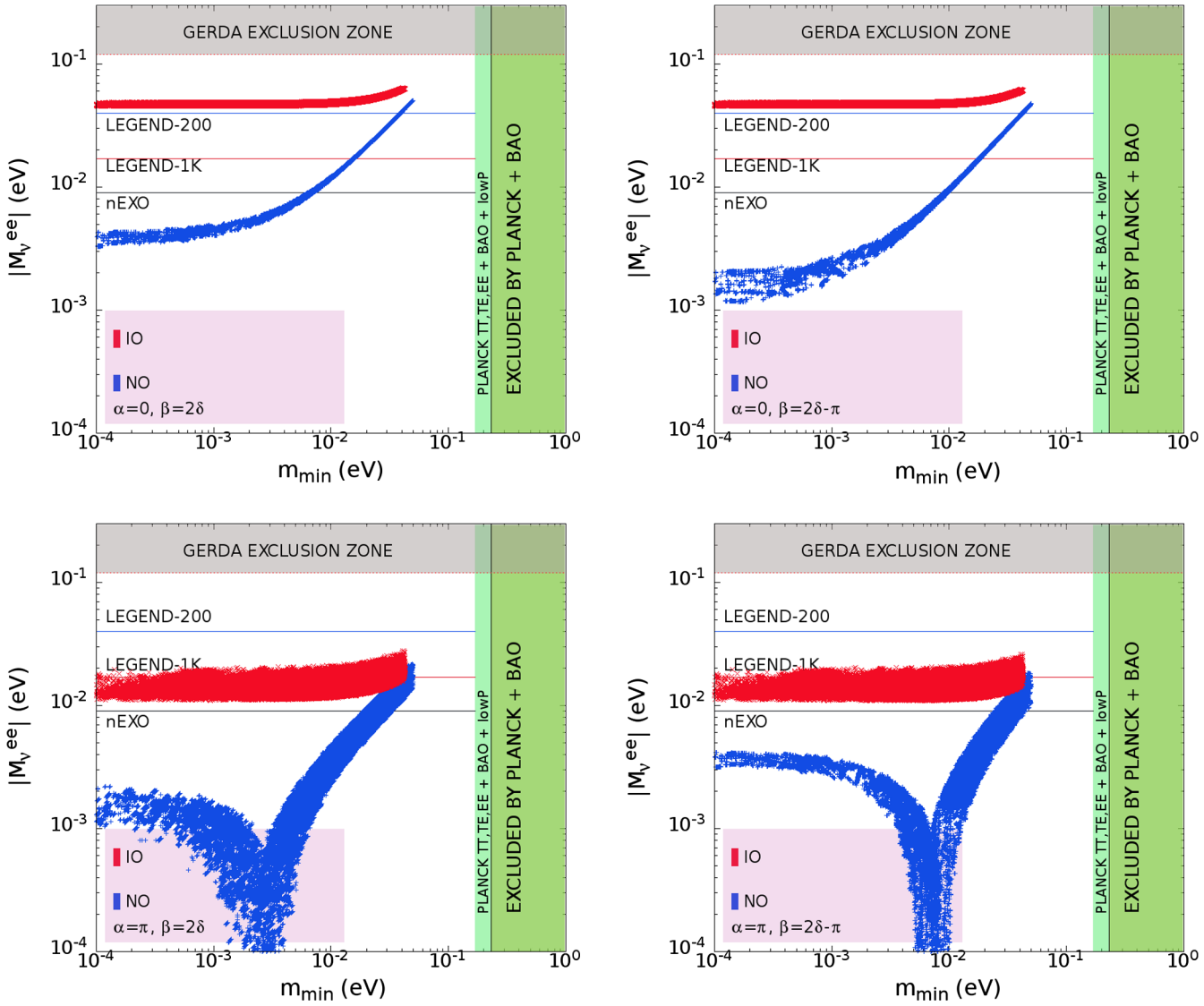

FIG. 2. Plots of $|M_\nu^{ee}|$ vs $m_{\min}$ for both types of mass ordering with four possible choices of the Majorana phases α and β. NO and IO refer to normal and inverted ordering respectively.

(ii) $|M_\nu^{ee}| = c_{12}^2 c_{13}^2 m_1 + s_{12}^2 c_{13}^2 m_2 - s_{13}^2 m_3$ for $\alpha = 0$, $\beta = 2\delta - \pi$,

(iii) $|M_\nu^{ee}| = c_{12}^2 c_{13}^2 m_1 - s_{12}^2 c_{13}^2 m_2 + s_{13}^2 m_3$ for $\alpha = \pi$, $\beta = 2\delta$ and

(iv) $|M_\nu^{ee}| = c_{12}^2 c_{13}^2 m_1 - s_{12}^2 c_{13}^2 m_2 - s_{13}^2 m_3$ for $\alpha = \pi$, $\beta = 2\delta - \pi$.

In $0\nu\beta\beta$ decay, M_ν^{ee} depends on α and $\beta - 2\delta$ [cf. Eq. (4.3)]. In a generic case, α and $\beta - 2\delta$ vary in the range $[0, 2\pi]$ (or $[-\pi, \pi]$, since angles are defined modulo 2π) to cover the largest possible parameter space. However, a notable feature of our scenario is that it uniquely fixes (i) α to be 0 or π and (ii) the combination $\beta - 2\delta$ to be 0 or $-\pi$ rather than the entire range of variation $[0, 2\pi]$ (or $[-\pi, \pi]$) as in a generic situation. This constraint tightly controls the range of variation of M_ν^{ee} and is implicitly reflected in the parameter space of $0\nu\beta\beta$ decay. The resulting plots of $|M_\nu^{ee}|$ vs the smallest mass eigenvalue $m_{\min}$ (m_1 for NO and m_3 for IO) are presented in Fig. 2 with significant upper limits on $|M_\nu^{ee}|$ for ongoing and future experiments. At the moment the most stringent exclusion zone on M_{ee} has been reported by the GERDA Phase II [26] experiment to be 0.12–0.26 eV depending on the value of the nuclear matrix element used. It is evident from Fig. 2 that $|M_{ee}|$ in each plot leads to an upper limit which is below the reach of the GERDA Phase II experimental data. The sensitivity reach of several other experiments such as LEGEND-200 (40 meV), LEGEND-1K (17 meV) and nEXO (9 meV) [27], shown in Fig. 2, can probe our model. In particular, if LEGEND-1K fails to observe a signal, the inverted mass ordering in our model corresponding to $\alpha = 0$ shall be excluded. Note that, for each case, the entire parameter space corresponding to the inverted mass ordering is likely to be ruled out for both $\alpha = 0$ and π if nEXO, covering its entire reach, does not observe any $\beta\beta0\nu$ signal.

TABLE V. Four possibilities for $A_{\mu e}$.

Possibilities	$\sin\delta$	$\cos\delta$
Case A	$+\sin\theta(\sin 2\theta_{23})^{-1}$	$+(\sin 2\theta_{23})^{-1}\sqrt{\cos^2\theta\sin^2 2\theta_{23}-\sin^2\theta\cos^2 2\theta_{23}}$
Case B	$-\sin\theta(\sin 2\theta_{23})^{-1}$	$+(\sin 2\theta_{23})^{-1}\sqrt{\cos^2\theta\sin^2 2\theta_{23}-\sin^2\theta\cos^2 2\theta_{23}}$
Case C	$+\sin\theta(\sin 2\theta_{23})^{-1}$	$-(\sin 2\theta_{23})^{-1}\sqrt{\cos^2\theta\sin^2 2\theta_{23}-\sin^2\theta\cos^2 2\theta_{23}}$
Case D	$-\sin\theta(\sin 2\theta_{23})^{-1}$	$-(\sin 2\theta_{23})^{-1}\sqrt{\cos^2\theta\sin^2 2\theta_{23}-\sin^2\theta\cos^2 2\theta_{23}}$

However, the latter exclusion is likely to be a generic feature of many models.

B. *CP* asymmetry in neutrino oscillations

Here we discuss the effect of the existence of leptonic Dirac *CP* violation δ in neutrino oscillation experiments. The phase δ makes its appearance in the *CP* asymmetry parameter A_{lm}, defined as

$$A_{lm}=\frac{P(\nu_l\to\nu_m)-P(\bar{\nu}_l\to\bar{\nu}_m)}{P(\nu_l\to\nu_m)+P(\bar{\nu}_l\to\bar{\nu}_m)}, \tag{4.4}$$

where $l,\ m=(e,\mu,\tau)$ are flavor indices and the P's are transition probabilities. The $\nu_\mu\to\nu_e$ transition probability is given by

$$P_{\mu e}\equiv P(\nu_\mu\to\nu_e)=P_{\rm atm}+P_{\rm sol}+2\sqrt{P_{\rm atm}}\sqrt{P_{\rm sol}}\cos(\Delta_{32}+\delta), \tag{4.5}$$

where $\Delta_{ij}=\Delta m^2_{ij}L/4E$ is the kinematic phase factor in which L denotes the baseline length and E represents the beam energy. The quantities $P_{\rm atm}$, $P_{\rm sol}$ are respectively defined as

$$\sqrt{P_{atm}}=\sin\theta_{23}\sin 2\theta_{13}\frac{\sin(\Delta_{31}-aL)}{(\Delta_{31}-aL)}\Delta_{31}, \tag{4.6}$$

$$\sqrt{P_{\rm sol}}=\cos\theta_{23}\sin 2\theta_{12}\frac{\sin aL}{aL}\Delta_{21}, \tag{4.7}$$

where $a=G_FN_e/\sqrt{2}$ with G_F being the Fermi constant and N_e being the electron number density in the medium of propagation which takes into account the matter effects in neutrino propagation through the Earth. An approximate value of a for the Earth is 3500 km^{-1}. In the limit $a\to 0$, Eq. (4.5) leads to the oscillation probability in vacuum. With this, the *CP* asymmetry parameter is given by

$$A_{\mu e}=\frac{P(\nu_\mu\to\nu_e)-P(\bar{\nu}_\mu\to\bar{\nu}_e)}{P(\nu_\mu\to\nu_e)+P(\bar{\nu}_\mu\to\bar{\nu}_e)}=\frac{2\sqrt{P_{\rm atm}}\sqrt{P_{\rm sol}}\sin\Delta_{32}\sin\delta}{P_{\rm atm}+2\sqrt{P_{\rm atm}}\sqrt{P_{\rm sol}}\cos\Delta_{32}\cos\delta+P_{\rm sol}} \tag{4.8}$$

where $\sin\delta$, given by Eq. (3.11), has two possible values and the same goes for $\cos\delta$. Hence there are two pairs of choices which give rise to two pairs of possibilities for $A_{\mu e}$ as given in Table V.

In Fig. 3 the *CP* asymmetry parameter $A_{\mu e}$, for both types of mass ordering, is plotted against the baseline

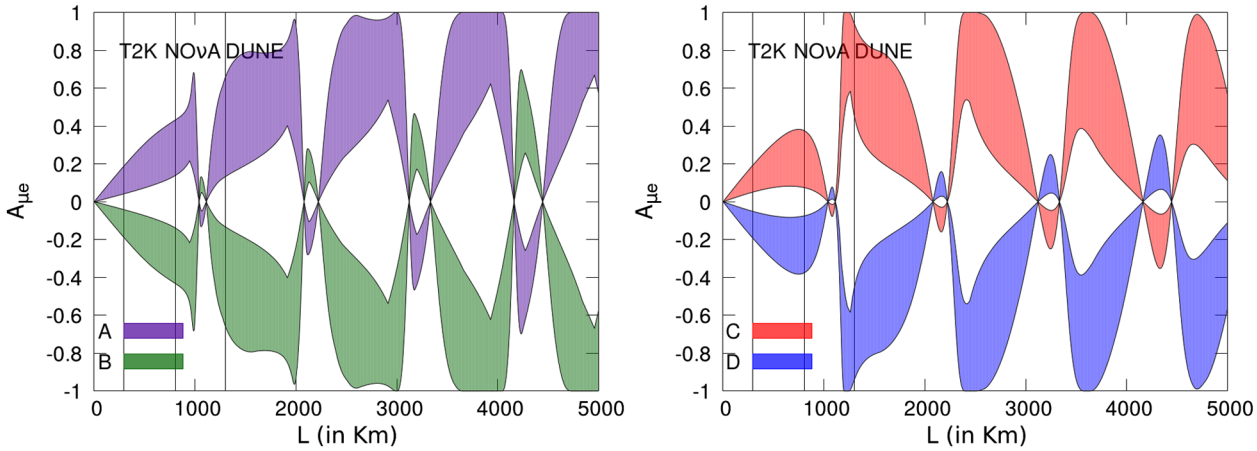

FIG. 3. *CP* asymmetry parameter $A_{\mu e}$ (for $E=1$ GeV), plotted against the baseline length L, for the four possibilities in Table V. Each plot stands for both NO and IO since numerically, within the 3σ range of θ_{23}, the two types of ordering are practically indistinguishable. The bands are due to θ_{23} and θ being allowed to vary within their experimental 3σ range and phenomenologically allowed range respectively with the other parameters kept at their best-fit values.

TABLE VI. Prediction of the ranges of $|A_{\mu e}|$ with $E = 1$ GeV.

Experiment	T2K	NOνA	DUNE
Cases A, B	0.04–0.18	0.14–0.44	0.14–0.64
Cases C, D	0.05–0.19	0.09–0.39	0.45–0.90

length L for four possibilities (Table V) and for a fixed beam energy ($E = 1$ GeV). The baseline lengths corresponding to experiments such as T2K, NOνA and DUNE are shown by vertical lines in the figure. For concreteness, Table VI provides the range of variation of the *CP*

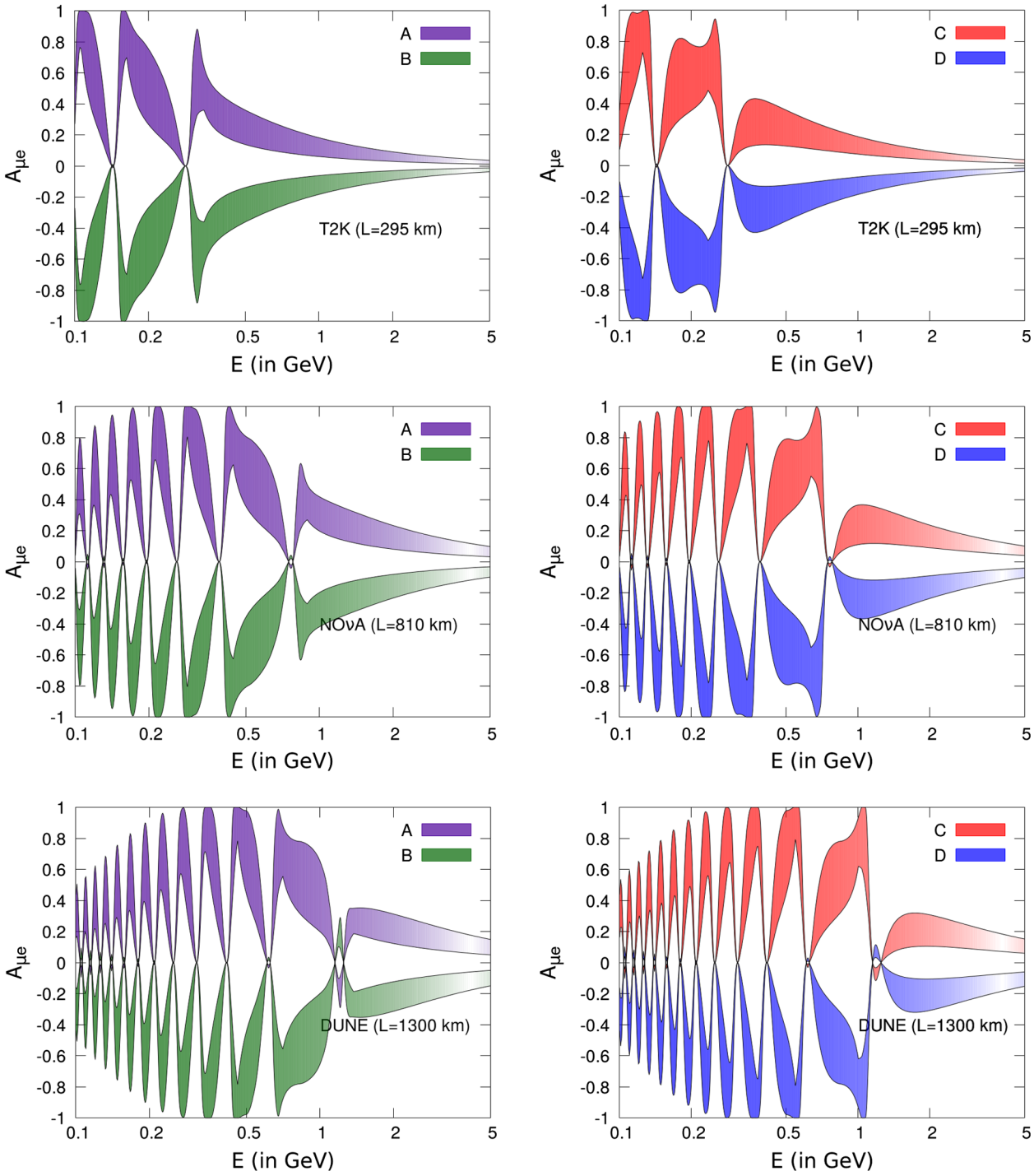

FIG. 4. Variation of the *CP* asymmetry parameter with beam energy E for different baselines lengths of $L = 295$, 810 and 1300 km corresponding to T2K, NOνA and DUNE respectively for both NO and IO; the numerical distinction between the two types of ordering is insignificant for the 3σ range of θ_{23}.

TABLE VII. Prediction of the ranges of $|A_{\mu e}|$ in T2K, NOνA, and DUNE.

T2K			
Energy	$E = 0.5$ GeV	$E = 1.0$ GeV	$E = 2.0$ GeV
Cases A, B	0.14–0.37	0.07–0.21	0.05–0.10
Cases C, D	0.14–0.37	0.06–0.19	0.05–0.10
NOνA			
Energy	$E = 0.5$ GeV	$E = 1.0$ GeV	$E = 2.0$ GeV
Cases A, B	0.31–0.80	0.21–0.43	0.08–0.24
Cases C, D	0.29–0.79	0.10–0.38	0.13–0.29
DUNE			
Energy	$E = 0.5$ GeV	$E = 1.0$ GeV	$E = 2.0$ GeV
Cases A, B	0.39–0.98	0.21–0.64	0.15–0.30
Cases C, D	0.41–0.97	0.61–0.87	0.13–0.32

asymmetry parameter $A_{\mu e}$ for a fixed energy of $E = 1$ GeV in T2K, NOνA and DUNE.

In Fig. 4, $A_{\mu e}$ is plotted against the beam energy E for four possible cases (Table V) separately for T2K, NOνA and DUNE for both types of mass ordering. In generating these plots, the atmospheric mixing angle θ_{23} has been taken to be within its currently allowed 3σ range while the remaining neutrino oscillation parameters have been kept fixed at their best-fit values. For each of these experiments, Table VII summarizes the allowed ranges of $A_{\mu e}$ for different values of the energy E.

C. Flavor flux ratios at neutrino telescopes

In order to discuss our predictions on the flavor flux ratios at neutrino telescopes (such as IceCube) we deem it necessary to first give a short review of the subject. The main source of ultra-high-energy cosmic neutrinos are pp and $p\gamma$ collisions[28]. In pp collisions, protons with energy in the TeV–PeV range produce neutrinos via the processes $\pi^+ \to \mu^+\nu_\mu$, $\pi^- \to \mu^-\bar{\nu}_\mu$, $\mu^+ \to e^+\nu_e\bar{\nu}_\mu$ and $\mu^- \to e^-\bar{\nu}_e\nu_\mu$. Therefore, the normalized flux distributions over different flavors are

$$\{\phi^S_{\nu_e}, \phi^S_{\bar{\nu}_e}, \phi^S_{\nu_\mu}, \phi^S_{\bar{\nu}_\mu}, \phi^S_{\nu_\tau}, \phi^S_{\bar{\nu}_\tau}\} = \phi_0\left\{\frac{1}{6}, \frac{1}{6}, \frac{1}{3}, \frac{1}{3}, 0, 0\right\}, \tag{4.9}$$

where the superscript S denotes the "source" and ϕ_0 denotes the overall flux normalization. For $p\gamma$ collisions, one is dealing with relatively less energetic γ rays (1–10^2 GeV range). Therefore, the center-of-mass energy of the γp system can barely allow the reactions $\gamma p \to \Delta^+ \to \pi^+ n$ and $\pi^+ \to \mu^+\nu_\mu$, $\mu^+ \to e^+\nu_e\bar{\nu}_\mu$. The corresponding normalized flux distributions over flavors are

$$\{\phi^S_{\nu_e}, \phi^S_{\bar{\nu}_e}, \phi^S_{\nu_\mu}, \phi^S_{\bar{\nu}_\mu}, \phi^S_{\nu_\tau}, \phi^S_{\bar{\nu}_\tau}\} = \phi_0\left\{\frac{1}{3}, 0, \frac{1}{3}, \frac{1}{3}, 0, 0\right\}. \tag{4.10}$$

In either case, if we take $\phi^S_l = \phi^S_{\nu_l} + \phi^S_{\bar{\nu}_l}$ with $l = e, \mu, \tau$,

$$\{\phi^S_e, \phi^S_\mu, \phi_\tau\} = \phi_0\left\{\frac{1}{3}, \frac{2}{3}, 0\right\}. \tag{4.11}$$

Since neutrino oscillations will change flavor distributions from the source (S) to the telescope (T) [29], the flux reaching the telescope is given by

$$\phi^T_l \equiv \phi^T_{\nu_l} + \phi^T_{\bar{\nu}_l} = \sum_m [\phi^S_{\nu_m} P(\nu_m \to \nu_l) + \phi^S_{\bar{\nu}_m} P(\bar{\nu}_m \to \bar{\nu}_l)]. \tag{4.12}$$

Given that the source-to-telescope distance is much greater than the oscillation length, the flavor oscillation probability can be averaged over many oscillations. Hence we have

$$P(\nu_m \to \nu_l) = P(\bar{\nu}_m \to \bar{\nu}_l) \approx \sum_i |U_{li}|^2 |U_{mi}|^2. \tag{4.13}$$

Thus the flux reaching the telescope, after using Eq. (4.11), will be

$$\begin{aligned}\phi^T_l &= \sum_i \sum_m \phi^S_m |U_{li}|^2 |U_{mi}|^2 \\ &= \frac{\phi_0}{3} \sum_i |U_{li}|^2 (|U_{ei}|^2 + 2|U_{\mu i}|^2).\end{aligned} \tag{4.14}$$

Using the unitarity of the PMNS matrix i.e., $|U_{ei}|^2 + |U_{\mu i}|^2 + |U_{\tau i}|^2 = 1$, we have

$$\begin{aligned}\phi^T_l &= \frac{\phi_0}{3}\left[1 + \sum_i |U_{li}|^2 (|U_{\mu i}|^2 - |U_{\tau i}|^2)\right] \\ &= \frac{\phi_0}{3}\left[1 + \sum_i |U_{li}|^2 \Delta_i\right],\end{aligned} \tag{4.15}$$

where $\Delta_i = |U_{\mu i}|^2 - |U_{\tau i}|^2$. If there is exact CP-transformed $\mu\tau$ (anti)symmetry, $\Delta_i = 0$, and $\phi^T_e = \phi^T_\mu = \phi^T_\tau$.

With the above background, one can define certain flavor flux ratios R_l ($l = e, \mu, \tau$) at the neutrino telescope as

$$R_l \equiv \frac{\phi^T_l}{\sum_m \phi^T_m - \phi^T_l} = \frac{1 + \sum_i |U_{li}|^2 \Delta_i}{2 - \sum_i |U_{li}|^2 \Delta_i}, \tag{4.16}$$

where $m = e, \mu, \tau$ and U is as in Eq. (2.3). Since $s^2_{13} \approx 0.01$, we can neglect $\mathcal{O}(s^2_{13})$ terms. Then the approximate expressions for the flux ratios become

$$R_e \equiv \frac{\phi_e^T}{\phi_\mu^T + \phi_\tau^T} \approx \frac{1 + \frac{1}{2}\sin^2 2\theta_{12}\cos 2\theta_{23} + \frac{1}{2}\sin 4\theta_{12}\sin 2\theta_{23}s_{13}\cos\delta}{2 - \frac{1}{2}\sin^2 2\theta_{12}\cos 2\theta_{23} - \frac{1}{2}\sin 4\theta_{12}\sin 2\theta_{23}s_{13}\cos\delta}, \tag{4.17}$$

$$R_\mu \equiv \frac{\phi_\mu^T}{\phi_e^T + \phi_\tau^T} \approx \frac{1 + \{c_{23}^2(1 - \frac{1}{2}\sin^2 2\theta_{12}) - s_{23}^2\}\cos 2\theta_{23} - \frac{1}{4}\sin 4\theta_{12}\sin 2\theta_{23}s_{13}\cos\delta(4c_{23}^2 - 1)}{2 - \cos^2 2\theta_{23} + \frac{1}{2}\sin^2 2\theta_{12}\cos 2\theta_{23}c_{23}^2 + \frac{1}{4}(3 - 4s_{23}^2)\sin 4\theta_{12}\sin 2\theta_{23}s_{13}\cos\delta}, \tag{4.18}$$

$$R_\tau \equiv \frac{\phi_\tau^T}{\phi_e^T + \phi_\mu^T} \approx \frac{1 + \{s_{23}^2(1 - \frac{1}{2}\sin^2 2\theta_{12}) - c_{23}^2\}\cos 2\theta_{23} - \frac{1}{4}\sin 4\theta_{12}\sin 2\theta_{23}s_{13}\cos\delta(4s_{23}^2 - 1)}{2 + \cos^2 2\theta_{23} + \frac{1}{2}\sin^2 2\theta_{12}\cos 2\theta_{23}c_{23}^2 + \frac{1}{4}(3 - 4c_{23}^2)\sin 4\theta_{12}\sin 2\theta_{23}s_{13}\cos\delta}. \tag{4.19}$$

Note that each R_l depends on $\cos\delta$ which from Eq. (3.11) is given by

$$\cos\delta = \pm\left(\sqrt{\cos^2\theta\sin^2 2\theta_{23} - \sin^2\theta\cos^2 2\theta_{23}}\right)\Big/ \sin 2\theta_{23}. \tag{4.20}$$

With $\theta = \pi/2 + \epsilon$ for any arbitrary ϵ, positive or negative, we can write

$$\cos\delta = \pm\left(\sqrt{\sin^2\epsilon\sin^2 2\theta_{23} - \cos^2\epsilon\cos^2 2\theta_{23}}\right)\Big/ \sin 2\theta_{23} \tag{4.21}$$

which is the same whether ϵ is positive or negative. For either sign, this explains why each R_l in Figs. 5 and 6 is symmetric about $\theta = \pi/2$ though the allowed range of θ is not (Table II). The "±" sign in Eq. (4.21) tells us that for a fixed θ (equivalently, for a fixed ϵ), and fixed θ_{23}, each R_l is double-valued except for $\theta = \pi/2$ (i.e., $\epsilon = 0$) where $\cos\delta = 0$ from Eqs. (4.21) and (3.11). However, instead of two discrete values of R_l, a continuous band is obtained for a fixed θ since θ_{23} has been allowed to vary in its current 3σ range while the other mixing angles are held fixed at their best-fit values. In the figure below, we plot the variation of the flavor flux ratios R_l with the $\mu\tau$ mixing parameter θ in its allowed range for both normal and inverted types of mass ordering. Unlike the CP asymmetry parameter in neutrino oscillation experiments, these flavor flux ratios are different for NO and IO, specifically in the allowed ranges of θ. An exact CP-transformed $\mu\tau$ interchange ($CP^{\mu\tau}$) antisymmetry leads to $R_e = R_\mu = R_\tau = 1/2$

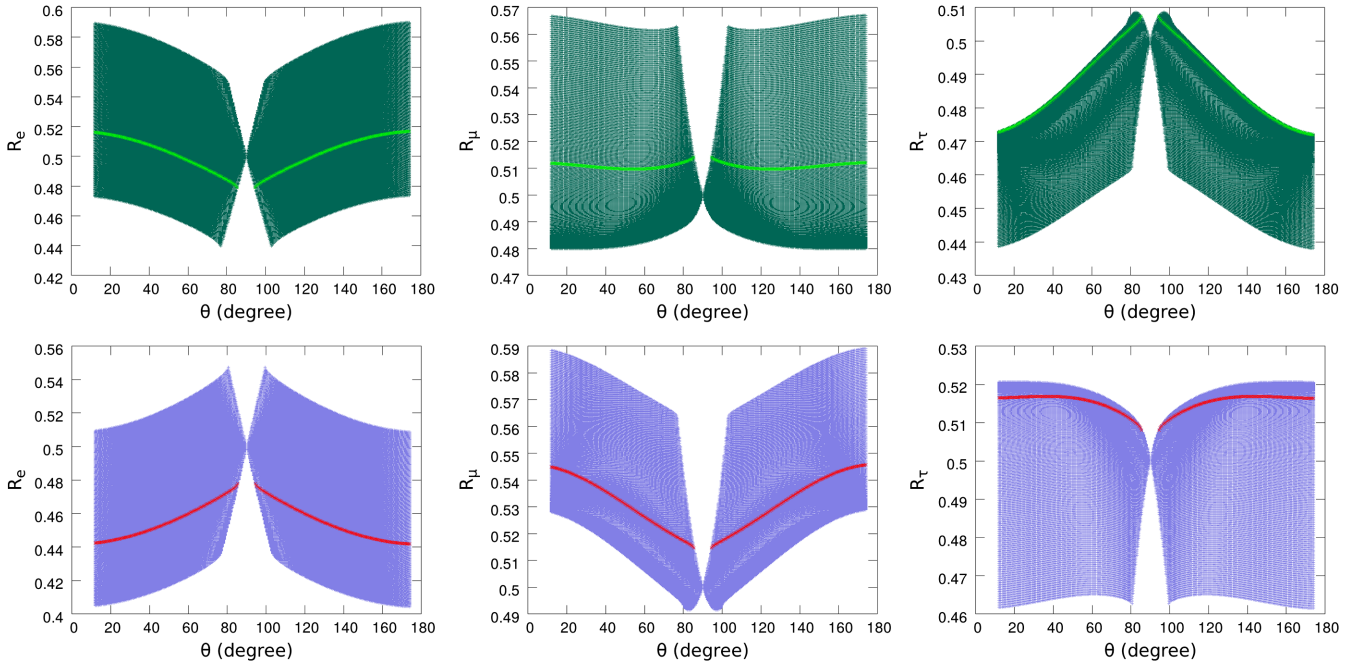

FIG. 5. Flux ratios R_e, R_μ, R_τ vs the $\mu\tau$-mixing parameter θ for normal ordering, where the three mixing angles have been allowed to vary over their 3σ ranges. The green (red) line in each plot of the upper (lower) panel corresponds to the best-fit value of the mixing angles. The plots in the upper (lower) panel correspond to $\cos\delta \geq 0$ (≤ 0).

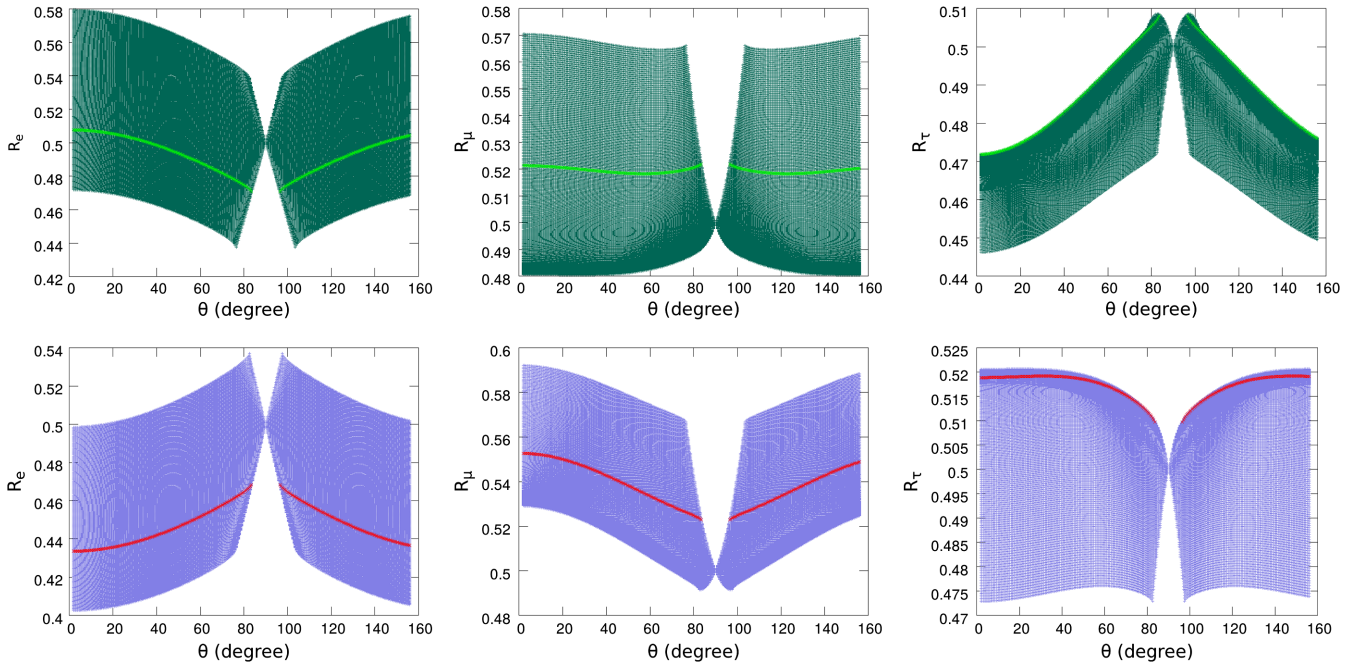

FIG. 6. Flux ratios R_e, R_μ, R_τ vs the $\mu\tau$-mixing parameter θ for inverted ordering where the three mixing angles have been allowed to vary over their 3σ ranges. The green (red) line in each plot of the upper (lower) panel corresponds to the best-fit value of the mixing angles. The plots in the upper (lower) panel correspond to $\cos\delta \geq 0$ (≤ 0).

irrespective of the mass ordering. This can be clearly seen from the approximate expressions of the flux ratios in Eqs. (4.17)–(4.19) in the limit $\theta = \pi/2$ or equivalently, $\theta_{23} = \pi/4$ and $\cos\delta = 0$. But a small deviation from $CP^{\mu\tau}$ (anti)symmetry may lead to a drastic change of the flux ratios as is clear from the sharp edges of the allowed parameter spaces on either side of $\theta = \pi/2$.

In order to obtain precise predictions for flavor flux ratios, a precise value of θ must be specified. In particular, precise measurements of δ and θ_{23} can be used to pinpoint a value of θ from Eq. (3.11). As an illustration, with the best-fit values of $\delta = 234^0$ (278°) and $\theta_{23} = 47.2°$ (48.1°) for NO (IO), the value of θ turns out to be 34.75° (75.9°). The contours corresponding to the best-fit values of the mixing angles are indicated in Figs. 5 and 6. Now, it can be clearly seen that, as θ deviates from $\pi/2$, the flavor flux ratios deviate drastically from 0.5 and the corresponding values have been tabulated in Table VIII. The quantitative predictions of the flux ratio θ deviating from $\pi/2$ are summarized in Table VIII. The current best-fit values are 215° (284°) for δ and 49.6° (49.8°) for θ_{23}, and thus θ is 34.75° (75.9°) for the NO (IO) case. The corresponding values of R_e, R_μ and R_τ have been found to be 0.456 (0.465), 0.529 (0.525) and 0.516 (0.512) respectively. It is interesting to note that while the predicted value of R_e is less than 0.5 those of R_μ and R_τ are greater than 0.5. If these best-fit values change in the future, the corresponding predictions for R_l can be easily obtained using the formulas (4.16) and (4.20) to test or falsify our proposal.

TABLE VIII. Prediction for the values of flux ratios (R_l) for $\theta \neq \pi/2$ [7].

Ordering↓	Best-fit value of δ	Best-fit value of θ_{23}	θ	R_e	R_μ	R_τ
NO	234°	47.2°	53.70°	0.456	0.529	0.516
IO	278°	48.1°	79.74°	0.465	0.525	0.512

V. SUMMARY AND CONCLUSIONS

We have proposed a *CP*-transformed mixed $\mu\tau$ antisymmetry in the light neutrino Majorana mass matrix M_ν implemented in the Lagrangian by a generalized *CP* transformation on left-chiral flavor neutrino fields. We explored its consequences in leptonic *CP* violation. The Dirac *CP* phase δ, which is in general nonmaximal, was found to be correlated with both the $\mu\tau$ mixing parameter θ and the atmospheric mixing angle θ_{23}. For a nonmaximal δ, one of the Majorana phases is neither zero nor π, thereby leading to a nonvanishing Majorana *CP* violation. Moreover, we discussed the consequences of our proposal on the $\beta\beta0\nu$ decay process in relation to ongoing and upcoming experiments. We have also investigated the quantitative variation of the *CP* asymmetry parameter $A_{\mu e}$ as a function of beam energy for different baseline lengths as appropriate for different experiments. We have further obtained the implications of $\mu\tau$ mixing on flavor flux ratios $R_{e,\mu,\tau}$ at neutrino telescopes such as IceCube.

While an exact $\mu\tau$ interchange antisymmetry leads to $R_e = R_\mu = R_\tau = 0.5$, any tiny departure will cause a significant deviation in the flux ratios, as has been explained quantitatively. Further, a careful measurement of these flux ratios in the future can put additional constraints on the parameter θ.

ACKNOWLEDGMENTS

We thank R. Samanta for useful discussions. The work of R. S. and A. G. is supported by the Department of Atomic Energy (DAE), Government of India. The work of P. R. has been supported by the Indian National Science Academy.

[1] S. F. King, J. Phys. G **42**, 123001 (2015).
[2] N. Aghanim *et al.* (Planck Collaboration), Astron. Astrophys. **596**, A107 (2016).
[3] K. Abe *et al.* (T2K Collaboration), Phys. Rev. Lett. **118**, 151801 (2017).
[4] P. Adamson *et al.* (NOvA Collaboration), Phys. Rev. Lett. **118**, 151802 (2017); **118**, 231801 (2017); A. Himmel (NOvA Collaboration), New neutrino oscillation results from NOVA (2018), https://indico.cern.ch/event/696410/.
[5] P. Adamson *et al.* (MINOS Collaboration), Phys. Rev. Lett. **110**, 251801 (2013); **110**, 171801 (2013).
[6] S.-H. Seo (RENO Collaboration), in *15th International Conference on Topics in Astroparticle and Underground Physics (TAUP 2017) Sudbury, Ontario, Canada, 2017* (2017), arXiv:1710.08204.
[7] I. Esteban, M. C. Gonzalez-Garcia, M. Maltoni, I. Martinez-Soler, and T. Schwetz, J. High Energy Phys. 01 (2017) 087.
[8] P. F. Harrison and W. G. Scott, Phys. Lett. B **547**, 219 (2002); W. Grimus and L. Lavoura, Phys. Lett. B **579**, 113 (2004); E. Ma, Phys. Lett. B **752**, 198 (2016); R. N. Mohapatra and C. C. Nishi, Phys. Rev. D **86**, 073007 (2012); J. High Energy Phys. 08 (2015) 092; S. F. Ge, D. A. Dicus, and W. W. Repko, Phys. Lett. B **702**, 220 (2011); Phys. Rev. Lett. **108**, 041801 (2012); R. Samanta, P. Roy, and A. Ghosal, Eur. Phys. J. C **76**, 662 (2016); R. Sinha, R. Samanta, and A. Ghosal, J. High Energy Phys. 12 (2017) 030.
[9] R. Samanta, R. Sinha, and A. Ghosal, arXiv:1805.10031; W. Grimus, A. S. Joshipura, S. Kaneko, L. Lavoura, H. Sawanaka, and M. Tanimoto, Nucl. Phys. **B713**, 151 (2005).
[10] G. Altarelli and F. Feruglio, Rev. Mod. Phys. **82**, 2701 (2010); H. Ishimori, T. Kobayashi, H. Ohki, Y. Shimizu, H. Okada, and M. Tanimoto, Prog. Theor. Phys. Suppl. **183**, 1 (2010); S. F. King, Prog. Part. Nucl. Phys. **94**, 217 (2017); S. T. Petcov, Eur. Phys. J. C **78**, 709 (2018); Nucl. Phys. **B892**, 400 (2015).
[11] R. N. Mohapatra and S. Nussinov, Phys. Rev. D **60**, 013002 (1999); T. Fukuyama and H. Nishiura, arXiv:hep-ph/9702253; C. S. Lam, Phys. Lett. B **507**, 214 (2001); E. Ma and M. Raidal, Phys. Rev. Lett. **87**, 011802 (2001); **87**, 159901(E) (2001); K. R. S. Balaji, W. Grimus, and T. Schwetz, Phys. Lett. B **508**, 301 (2001); A. Ghosal, Mod. Phys. Lett. A **19**, 2579 (2004); Z. z. Xing and Z. h. Zhao, Rep. Prog. Phys. **79**, 076201 (2016); S. F. Ge, H. J. He, and F. R. Yin, J. Cosmol. Astropart. Phys. 05 (2010) 017.
[12] F. P. An *et al.* (Daya Bay Collaboration), Phys. Rev. Lett. **115**, 111802 (2015).
[13] G. Ecker, W. Grimus, and H. Neufeld, J. Phys. A **20**, L807 (1987); W. Grimus and M. N. Rebelo, Phys. Rep. **281**, 239 (1997); R. N. Mohapatra and C. C. Nishi, Phys. Rev. D **86**, 073007 (2012); S. Gupta, A. S. Joshipura, and K. M. Patel, Phys. Rev. D **85**, 031903 (2012); F. Feruglio, C. Hagedorn, and R. Ziegler, J. High Energy Phys. 07 (2013) 027; M. Holthausen, M. Lindner, and M. A. Schmidt, J. High Energy Phys. 04 (2013) 122; M. C. Chen, M. Fallbacher, K. T. Mahanthappa, M. Ratz, and A. Trautner, Nucl. Phys. **B883**, 267 (2014); G. J. Ding, S. F. King, C. Luhn, and A. J. Stuart, J. High Energy Phys. 05 (2013) 084; G. J. Ding, S. F. King, and A. J. Stuart, J. High Energy Phys. 12 (2013) 006; G. J. Ding and Y. L. Zhou, J. High Energy Phys. 06 (2014) 023; G. J. Ding and S. F. King, Phys. Rev. D **89**, 093020 (2014); C. C. Li and G. J. Ding, Nucl. Phys. **B881**, 206 (2014); S. F. King and T. Neder, Phys. Lett. B **736**, 308 (2014); C. C. Li and G. J. Ding, J. High Energy Phys. 05 (2015) 100; G. J. Ding and Y. L. Zhou, Chin. Phys. C **39**, 021001 (2015); F. Feruglio, C. Hagedorn, and R. Ziegler, Eur. Phys. J. C **74**, 2753 (2014); A. Di Iura, C. Hagedorn, and D. Meloni, J. High Energy Phys. 08 (2015) 037; C. Hagedorn, A. Meroni, and E. Molinaro, Nucl. Phys. **B891**, 499 (2015); P. Chen, C. Y. Yao, and G. J. Ding, Phys. Rev. D **92**, 073002 (2015); C. C. Nishi, Phys. Rev. D **93**, 093009 (2016); C. C. Nishi and B. L. Snchez-Vega, J. High Energy Phys. 01 (2017) 068; W. Rodejohann and X. J. Xu, Phys. Rev. D **96**, 055039 (2017); I. Girardi, A. Meroni, S. T. Petcov, and M. Spinrath, J. High Energy Phys. 02 (2014) 050; J. T. Penedo, S. T. Petcov, and A. V. Titov, J. High Energy Phys. 12 (2017) 022; L. L. Everett, T. Garon, and A. J. Stuart, J. High Energy Phys. 04 (2015) 069; L. L. Everett and A. J. Stuart, Phys. Rev. D **96**, 035030 (2017); A comprehensive review: S. F. King, Prog. Part. Nucl. Phys. **94**, 217 (2017).
[14] P. Chen, G. J. Ding, F. Gonzalez-Canales, and J. W. F. Valle, Phys. Lett. B **753**, 644 (2016).
[15] S. F. King and C. C. Nishi, Phys. Lett. B **785**, 391 (2018); S. F. King and Y. L. Zhou, arXiv:1901.06877.
[16] R. Samanta, P. Roy, and A. Ghosal, J. High Energy Phys. 06 (2018) 085.
[17] W. Grimus, S. Kaneko, L. Lavoura, H. Sawanaka, and M. Tanimoto, J. High Energy Phys. 01 (2006) 110.
[18] A. S. Joshipura, J. High Energy Phys. 11 (2015) 186; A. S. Joshipura and N. Nath, Phys. Rev. D **94**, 036008 (2016).
[19] A. S. Joshipura and K. M. Patel, Phys. Lett. B **749**, 159 (2015).
[20] M. Tanabashi *et al.* (Particle Data Group), Phys. Rev. D **98**, 030001 (2018).

[21] J. Bernabeu, G. C. Branco, and M. Gronau, Phys. Lett. **169B**, 243 (1986); G. C. Branco, L. Lavoura, and M. N. Rebelo, Phys. Lett. B **180**, 264 (1986).

[22] G. C. Branco, L. Lavoura, and J. P. Silva, *CP Violation* (Clarendon Press, Oxford, 1999); J. Iizuka, Y. Kaneko, T. Kitabayashi, N. Koizumi, and M. Yasue, Phys. Lett. B **732**, 191 (2014); R. Samanta and A. Ghosal, Nucl. Phys. **B911**, 846 (2016); R. Samanta, M. Chakraborty, and A. Ghosal, Nucl. Phys. **B904**, 86 (2016).

[23] M. H. Rahat, P. Ramond, and B. Xu, Phys. Rev. D **98**, 055030 (2018).

[24] B. Adhikary, M. Chakraborty, and A. Ghosal, J. High Energy Phys. 10 (2013) 043; 09 (2014) 180(E).

[25] W. Rodejohann, Int. J. Mod. Phys. E **20**, 1833 (2011); P. S. Bhupal Dev, S. Goswami, M. Mitra, and W. Rodejohann, Phys. Rev. D **88**, 091301 (2013).

[26] M. Agostini *et al.* (GERDA Collaboration), Phys. Rev. Lett. **120**, 132503 (2018).

[27] M. Agostini, G. Benato, and J. A. Detwiler, Phys. Rev. D **96**, 053001 (2017).

[28] R. Gandhi, C. Quigg, M. H. Reno, and I. Sarcevic, Astropart. Phys. **5**, 81 (1996); R. Gandhi, C. Quigg, M. H. Reno, and I. Sarcevic, Phys. Rev. D **58**, 093009 (1998).

[29] Z. Z. Xing and S. Zhou, Phys. Rev. D **74**, 013010 (2006); W. Rodejohann, J. Cosmol. Astropart. Phys. 01 (2007) 029; Z. z. Xing, Phys. Lett. B **716**, 220 (2012).